Hydrogen bond surrogate stabilized water soluble 3_{10}-Helix froma disordered pentapeptide containing codedα-amino acids

Sunit Pal, Erode N. Prabhakaran

PII: S0040-4039(18)30628-2
DOI: https://doi.org/10.1016/j.tetlet.2018.05.029
Reference: TETL 49976

To appear in: *Tetrahedron Letters*

Received Date: 26 February 2018
Revised Date: 10 May 2018
Accepted Date: 13 May 2018

Please cite this article as: Pal, S., Prabhakaran, E.N., Hydrogen bond surrogate stabilized water soluble 3_{10}-Helix froma disordered pentapeptide containing codedα-amino acids, *Tetrahedron Letters* (2018), doi: https://doi.org/10.1016/j.tetlet.2018.05.029

Graphical Abstract

To create your abstract, type over the instructions in the template box below.
Fonts or abstract dimensions should not be changed or altered.

Hydrogen bond surrogate stabilized water soluble 3_{10}-Helix from a disordered pentapeptide containing coded α-amino acids

Sunit Pal, Erode. N. Prabhakaran*

Leave this area blank for abstract info.

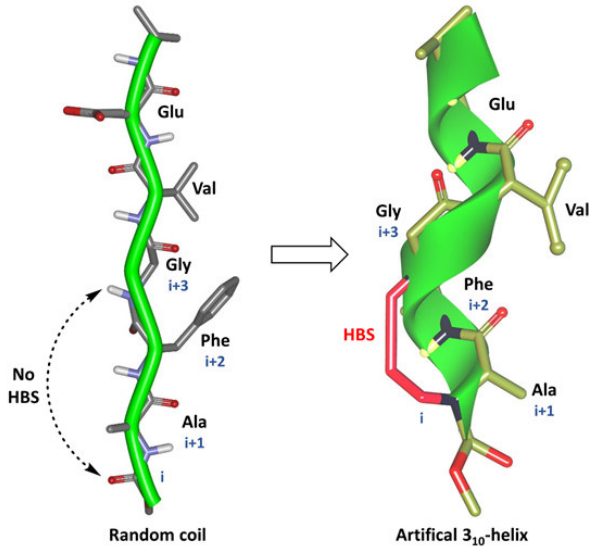

ELSEVIER

Tetrahedron Letters
journal homepage: www.elsevier.com

Hydrogen bond surrogate stabilized water soluble 3_{10}-Helix from a disordered pentapeptide containing coded α-amino acids

Sunit Pal, Erode N. Prabhakaran*

Department of Organic Chemistry, Indian Institute of Science, Karnataka, Bangalore, India – 560 012.

ARTICLE INFO

Article history:
Received
Received in revised form
Accepted
Available online

Keywords:
HBS
3_{10}-helix
ROE
Random coil
C^{α}-tetrasubstituted α-amino acids

ABSTRACT

Replacing a hypothetical i+3→i peptide H-bond in a disordered pentapeptide, that lacks any helicogenic C^{α}-tetrasubstituted residues, with a propyl linker and carbamylating the N-terminal nitrogen constrains it in the elusive 3_{10}-helical structure with high helicity and stability under varying conditions of temperature and pH, confirmed by NMR and CD analyses.

3_{10}-Helix is the second most abundant helical structure (10%)[1] in globular proteins next to the α-helix (90%) and contains the i+3→i intramolecular hydrogen bond between the backbone peptide N-H of the i+3[rd] residue and C=O of the i[th] residue (Figure 1). Although the (φ, ψ) backbone dihedral angles in 3_{10}-helices and α-helices fall in the same region of the Ramachandran plot,[1, 2] the 3_{10}-helices are less stable and typically shorter (3 to 7 residues)[3] due to unfavourable van der Waals clashes and strict linear arrangement of the i+3→i hydrogen bonds.[3-5] 3_{10}-helices are often found at the termini of α-helices and play important roles as nucleation sites for helix formation during protein folding.[6]

Over the years, there has been great interest in developing methods to constrain short peptides in helical conformations. Synthetic models to constrain peptides in to α-helix have primarily used two strategies: a) introducing a covalent surrogate for the main chain i+4→i H-bond (hydrogen bond surrogate, HBS, strategy)[7, 8]; and b) introducing covalent[9-13], non-covalent[14-16] or metal coordination[17] interactions between i[th] and i+4[th] side chains. Non-peptidic models have also been successful in mimicking α-helical surfaces.[18] For mimicking the structurally more challenging 3_{10}-helices, the latter methods of introducing i···i+3 side chain bridges, including lactam bridges[6], 1,2,3-triazole bridges[19], metathesis derived hydrocarbon bridges[20-22], photo- induced covalent bridges[23] and *p*-phenylenediacetic acid bridge[24], have been successful. The former strategy of introducing a covalent surrogate for the main chain i+3→i H-bond has however not yet been explored.

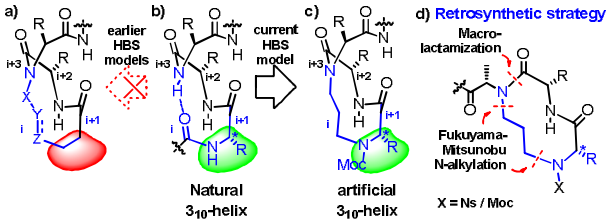

Figure 1. ChemDraw rendition of: a) earlier hydrogen bond surrogate (HBS) models highlighting their lack of the i+1[st] amino acid and N_{i+1}-CO group, hence deficient for constraining peptides in (b) the 3_{10}-helical conformation; c) current HBS model conserves the i+1[st] residue and N_{i+1}-CO group, hence stabilizes even a completely disordered pentapeptide in the elusive 3_{10}-helical conformation. d) Retrosynthesis involves two initial Fukuyama-Mitsunobu N-alkylation reactions followed by macrolactamization.

An important challenge about 3_{10}-helices is that, short peptides containing coded amino acids seldom form stable 3_{10}-helical structures outside their native protein context,[25] much lesser than those for α-helical structures.[26, 27] As a result C^{α}-tetrasubstituted amino acids such as α-aminoisobutyric acid (Aib), whose allowed (φ, ψ) angles are extremely small and perfectly match with those of 3_{10}- and α-helices,[1, 2, 28, 29] have been extensively incorporated (50% to 100%)[30, 31] in peptide sequences to constrain them into 3_{10}-helical structures.[2, 11, 32] In fact, this is done in addition to introduction of other side chain constraints.[21, 22] Such peptides hence suffer from poor solubility in water owing to their large apolar aliphatic surfaces and require specially designed C^{α}-tetrasubstituted α-amino acids functionalized with polar side chains to improve water solubility.[33] The steric bulk at

* Corresponding author. Tel.: +91-80-2293-3380; fax: +91-80-2360-0529; e-mail: erodeprabhakaran02@gmail.com

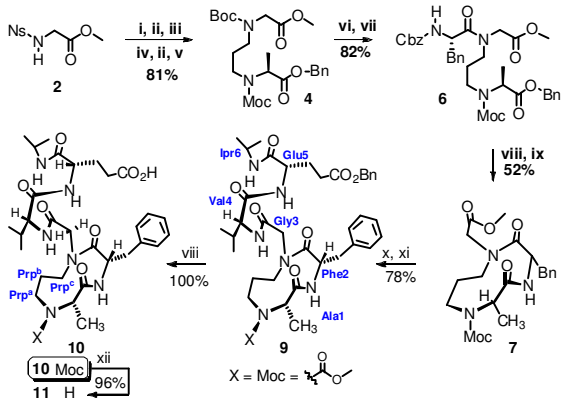

Legend: (i) PPh_3, DIAD, THF, 1,3-propanediol; (ii) PhSH, K_2CO_3, CH_3CN; (iii) $(Boc)_2O$, K_2CO_3, dioxane:H_2O; (iv) Ns-Ala-OBn (3), PPh_3, DIAD, THF; (v) Moc-Cl, K_2CO_3, CH_2Cl_2; (vi) TFA, CH_2Cl_2; (vii) Cbz-Phe-OH (5), ECF, NMM, THF;(viii) Pd/C/H_2, MeOH; (ix) EDC, HOBT, DIPEA, CH_3CN; (x) Li-OH,MeOH:H_2O; (xi)TFA-Val-Glu(OBn)-NHiPr (8), EDC, HOBT, DIPEA, CH_3CN; (xii) HBr/AcOH. Boc, tert-butyloxycarbonyl; Bn, benzyl; Ns, o-nitrobenzenesulfonyl; Moc, methyloxy carbonyl; Ipr, isopropylamine.

Scheme11. Synthesis of the HBS-constrained 3_{10}-helix Moc-cyclo[Ala^1-Phe^2]-Gly^3-Val^4-Glu^5-Ipr^6 (**10**). cyclo[Ala^1-Phe^2]-Gly^3 denotes the propyl cross linker between N_{Ala1} and N_{Gly3}. The methylene groups of the propyl linker are labelled Prp^a, Prp^b, Prp^c from N- to C-terminus of **10**.conservation of which may prove crucial to mimicking and stabilizing the more stringent 3_{10}-helix.

C^α of the C^α-tetrasubstituted α-amino acids also encumber their backbone peptide bonds, which are crucial recognition elements, from being approached by molecules for interactions.

We envisioned the design of the first H-bond surrogate (HBS) (Figure 1b) that can replace the main chain i+3→i H-bond, as a valuable method for stabilizing a short disordered peptide – that is devoid of C^α-tetrasubstituted amino acid residues – into 3_{10}-helix. As mentioned earlier, the HBS strategy,[7, 34] (Figure 1a) has been successful in constraining short, natural α-amino acid containing peptides into biologically relevant α-helical (n = 4)[35] and π- helical (n = 5)[36] conformations. But the 3_{10}-helical (n = 3) structures (Figure 1b) have not been accessible by this method yet. Examination of the two earlier HBS models[7, 34] revealed that the i+1st residue (Figure 1a) is not conserved in them. The backbone groups (-NH-C^αR-) of the i+1st residue get replaced by achiral groups (e.g. -CH_2-CH_2-), resulting in loss of crucial natural recognition elements and structural constraints.

Here we design a novel HBS model (Figure 1c) where both these important structural elements (N and C^αR) of the i+1st amino acid are conserved. The N-terminal i+3→i hydrogen bond (>N-H…O=CR-N<) is replaced with a propyl surrogate (>N-CH_2-CH_2-CH_2-N<) and a carbamyl group planarizes the i+1st nitrogen. An efficient synthetic strategy is designed to incorporate this HBS model in a short disordered pentapeptide Boc-Ala^1-Phe^2-Gly^3-Val^4-Glu^5-Ipr^6 (**1**) (Ipr is isopropylamide), which is devoid of C^α-tetrasubstituted amino acids. Extensive 2D NMR and circular dichroism (CD) spectral analyses reveal that the current HBS-constrained peptide **10**, is uniquely restricted in a robust water-soluble 3_{10}-helix which is stable at different pHs and temperatures in spite of the absence of C^α-tetrasubstituted amino acids. Current method will provide access to 3_{10}-helical mimics with exclusively coded amino acid side chains in its sequence.

1 has an order-breaking Gly residue and lacks any C^α-tetrasubstituted amino acids that promote 3_{10}-helix. AGADIR[37] calculations confirmed the lack of any helical structure in **1** (0.02% helicity) (S7.2). Any gain in 3_{10}-helicity in Moc-cyclo[Ala^1-Phe^2]-Gly^3-Val^4-Glu^5-Ipr^6 (**10**) (Scheme 1), the HBS constrained mimic of **1**, will hence be owing to the HBS-cross link in it.

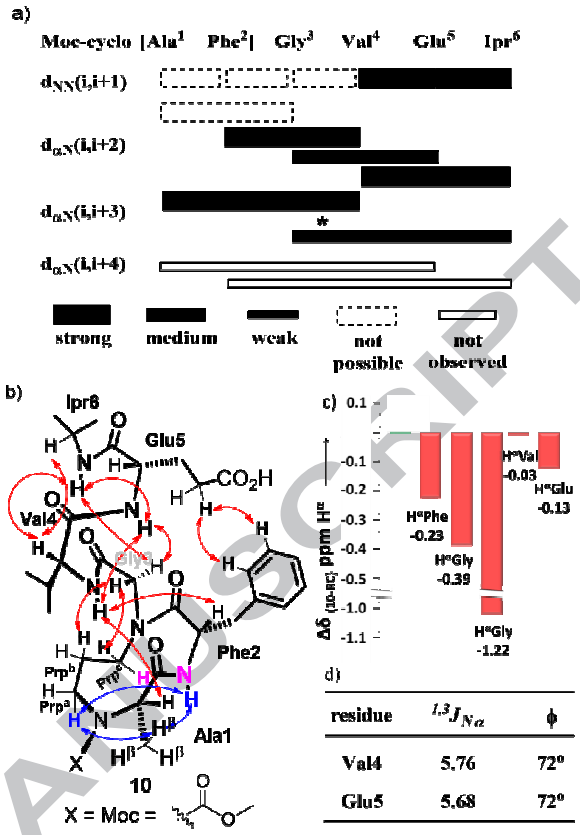

Figure22. a) ROE correlation chart for **10** showing sequential cross-peaks characteristic of 3_{10}-helical conformation in all its residues. Rectangular bars indicate ROE cross peak relative intensities. The Ala and Gly residues lack the backbone NH and hence the corresponding ROEs are not possible (S5.21.). b) The ChemDraw rendition of **10** representing all the key ROEs (10% D_2O/H_2O) that establish the 3_{10}-helical structure in it. c) Bar plot showing the negative secondary chemical shifts of H^α of residues in **10** from corresponding random coil (RC) values ($\Delta\delta_{10\text{-}RC}H^\alpha$ ppm). d) Table of $^{1,3}J_{\alpha N}$ values and corresponding φ dihedral angles for Val4, Glu5 in **10** (S5.25).

In order to test the propensity of the Novel HBS to stabilize **1** in 3_{10}-helical conformation, we synthesized **10** (Scheme 1). Two Fukuyama-Mitsunobu reactions[38] using N-nosyl activated aminoesters **2** and **3** placed the propyl linker between the nitrogen atoms of Ala and Gly residues. The N-nosyl groups were replaced by Boc / Moc (**4**), which were better amenable to peptide coupling conditions. Boc-deprotection of **4** and coupling with **5** gave **6**. Reductive double deprotection of Cbz and Bn ester in **6** and macrolactamization yielded **7**. Ester deprotection of **7** and coupling with **8** gave C-terminal extended **9**. Reduction of side chain benzyl ester in **9** yielded **10**.

10 is water soluble. There are two segments in **10**: a) the HBS-constrained cyclic segment, Moc-cyclo[Ala^1-Phe^2], intended for 3_{10}-helix-nucleation; and b) the acyclic segment Gly^3-Val^4-Glu^5-Ipr^6 for propagation of one 3_{10}-helical cycle at its C-terminus. The solution structure of either segment in **10** was established by 2D NMR and circular dichroism (CD) spectral analyses (10% D_2O in H_2O) and molecular dynamic simulation analyses. First, 2D TOCSY and HSQC spectra were used to assign all the ^1H, ^{13}C NMR signals (S5.15, 16.) and ROE cross peaks (S5.17, 22.).

In the cyclic segment of **10** three key ROE constraints ($H^N_{Phe2}\cdots H_{Prpa}$; $H^\beta_{Ala1}\cdots H_{Prpa}$ and $H^N_{Phe2}\cdots H^\beta_{Ala1}$) (blue arrows in Figure 2b) establish a triad interaction involving H^N_{Phe2} and one each of the H^β_{Ala1} and H_{Prpa} nuclei (S5.17, 18). This is consistent with a slight shift (0.03 ppm) in one of the H^β_{Ala1} signals from the other two H^β_{Ala1} signals (^1H NMR) (S5.17, 18.). Such a shift between the two $H_{Prp}{}^a$s is immeasurable but is apparent in the

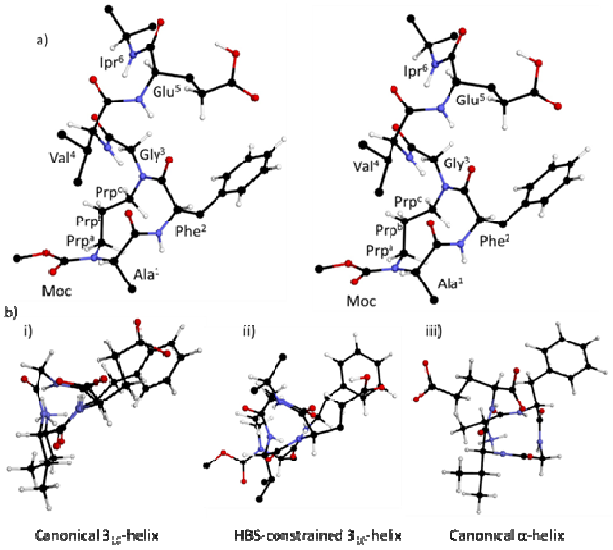

c)

residue	ϕ	ψ
Ala^1	-	-40
Phe^2	-47	-30
Gly^3	-73	-15
Val^4	-70	-20
Glu^5	-74	-3

d)

3$_{10}$-Helix model	ϕ	ψ
n poly Ala[20]	-57	-30
by Perutz[26]	-49	-26
n proteins[2,b]	-71	-18
in proteins[4]	-69	-18

Figure 3. a) Streoview of energy minimized structure of **10,** consistent with the ROE constraints (10% D_2O/H_2O). Select hydrogens involved in key ROEs are shown. b) The helix-axis views of, i) canonical 3$_{10}$-helix (of AFGVE); ii) the simulated helical fold in HBS-constrained **10**; and iii) canonical α-helix (of AFGVE). c) List of (φ,ψ) dihedral angles of the five residues in the simulated structure of **10,** consistent with, d) the (φ,ψ) values reported in different 3$_{10}$-helical models.(S5.21)

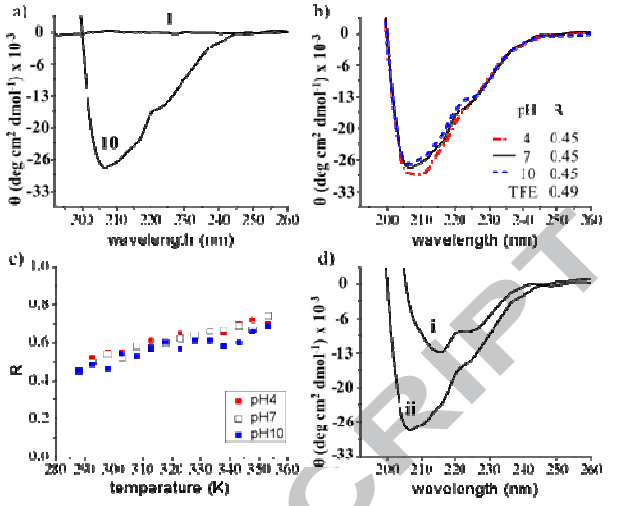

Figure 4. a) CD spectra of **1** and **10** in pH 7 (30 mM phosphate) buffer. b) Effect of pH (pH 4, 30 mM acetate buffer; pH 7, 30 mM phosphate buffer; pH 10, 30 mM carbonate buffer) on the CD spectrum of **10**. c) Effect of temperature on the ratio R (= $\theta_{n\rightarrow\pi^*}/\theta_{\pi\rightarrow\pi^*}$) of **10**. d) CD spectra of (i) **11** and (ii) **10** in pH 7 (30 mM phosphate) buffer.

smooth broadness of this signal, unlike the relatively sharp multiplets observed for both its neighbors $H_{prp}{}^c$ and $H_{Prp}{}^b$. These constraints are consistent with a Type III β- turn (3$_{10}$-helical)[3, 31, 39] structure in the cyclic segment, with Ala1 and Phe2 snuggly occupying i+1, i+2 positions. The exo-cyclic Moc group is oriented perpendicular to the imaginary helix axis (Ala1, Phe2 carbonyl orientations).

In the acyclic segment, consecutive $d_{NN}(i,i+1)$; $d_{\alpha N}(i,i+2)$ and $d_{\alpha N}(i,i+3)$ ROE cross peaks (Figure 2a) (S5.19,20.) are observed,[34] which are diagnostic of 3$_{10}$-helical[33] fold. The only exception is the $d_{\alpha N}$(Phe2,Glu5) cross peak which is not visible because the H^{α}_{Phe2} signal gets partially decoupled during water suppression and is also merged with H^{α}_{Ala1} (4.45 ppm). The observance of inter-side chain $H^{Aro}_{Phe2}\cdots H^{\gamma}_{Glu5}$ ROE (Figure 2b) (S5.22.) however confirms the desirable Phe2···Glu5 proximity. Additionally, the C-terminal Ipr6 exhibits four ROEs ($H^{\alpha}_{Ipr6}\cdots H^{\alpha}_{Val4}$, $H^{N}_{Ipr6}\cdots H^{\alpha}_{Val4}$, $H^{N}_{Ipr6}\cdots H^{N}_{Glu5}$, $H^{N}_{Ipr6}\cdots H^{\alpha}_{Gly3}$) establishing a compact 3$_{10}$-helical fold without fraying at the C-terminus. The $H^{\alpha}_{Gly3}\cdots H_{Prp}{}^c$, $H^{\alpha}_{Gly3}\cdots H_{Prp}{}^b$ ROEs for one of the H^{α}s of Gly and $H^{\alpha}_{Gly3}\cdots H^{N}_{Glu5}$, $H^{\alpha}_{Gly3}\cdots H^{N}_{Ipr6}$ for the other, are consistent with a continuous 3$_{10}$-helical fold including at Gly3, such that there is little wiggling room away from it throughout the backbone in **10**. The absence of $d_{\alpha N}(i,i+4)$ (S5.19.) ROE cross peaks indicate the absence of α-helical folds that usually compete with 3$_{10}$-helices.[40]

The $\delta_{H\alpha}$ of Phe2 to Glu5 in **10** show negative secondary chemical shifts ($\Delta\delta_{\mathbf{10}\text{-RC}}$ ppm) (Figure 2c) from corresponding random coil (RC) $\delta_{H\alpha}$ values[41](S5.24). Similar shifts in the C^{α}-trisubstituted α-amino acid containing peptide ELLELDKWASLWN[25] have served as diagnostic indicators of a 3$_{10}$-helical fold in it. Note that $\delta_{H\alpha}$Ala1 cannot be similarly compared with RC values since Ala1 nitrogen is coupled to a exo-cyclic carbamate. Further, based on the Karplus equation[42] the $^{13}J_{N\alpha}$ coupling constant values for Val4 and Glu5 indicate that both the φ_{Val4} and φ_{Glu5} adopt 72° (Figure 2d) (S5.25), which are characteristic of 3$_{10}$-helical folds.[39, 43, 44]

The minimum energy structure of **10** was further computed using standard MD protocol applying the CHARMM force field in Discovery Studio (v 16.1), incorporating Fourteen ROESY-derived inter-proton distance constraints and the two (φ, ψ) dihedral angle constraints. The dihedral angles (Figure 3c) for all residues in the computed structure (Figure 3a) are consistent with the canonical values reported for 3$_{10}$-helical folds (Figure 3d).[3] The helix-axis view of the simulated structure of HBS-constrained **10** (Figure 3bii) highlights the relative orientations of its residues and peptide bonds and is clearly similar to the helix-axis view structure of canonical 3$_{10}$-helix (Figure 3bi) and not with that of canonical α-helix (Figure 3biii). Additionally, in both simulated and ball-and-stick (S5.18, S6.4) model structures of **10**, one of the H_{Prpc} protons faces towards H^{N}_{Phe2} while the other is exposed on the helix surface. This is consistent with the two geminal Hs in exclusively Prp^c (and not Prp^a or Prp^b) showing two distinct ^{1}H NMR signals (Δδ=0.32 ppm) (S5.17.). The NMR data thus indicated that the novel HBS linker constrains the cyclic segment of **10** in 3$_{10}$-helical conformation, which imposes a similar structure in the succeeding C-terminal acyclic peptide segment.

The 3$_{10}$-helical conformation of **10** was further confirmed by CD spectral data (S7). The CD spectrum of the negative control peptide **1** showed indiscernible minima close to θ = 0 (S7.2), confirming the lack of any ordered structure in it. CD spectrum of **10** (Figure 4a) revealed two negative λ minima at 207 nm and 224 nm in pH 4, 7 and 10 buffers, which are similar to $\lambda_{\pi\rightarrow\pi^*}$ and $\lambda_{n\rightarrow\pi^*}$ minima characteristic of helical folds in peptides (S7.5).[22, 33, 45] There is little variance in these λ_{min} values with change in pH (4, 7, 10) or temperature (288-353 K) (S7.7-9), indicating an unperturbed helical structure in **10** under varying conditions.

The ratio R (= $\theta_{n\rightarrow\pi^*}/\theta_{\pi\rightarrow\pi^*}$) which further reports on the nature of helical structure (≥1 = α-helix; <0.6 = 3$_{10}$-helix; 0.6-1 = mixture of both)[30, 33, 46] was consistently 0.45 (288 K) (Figure 4b) at these pHs (S7.12), indicating the remarkably pH-independent predominance of 3$_{10}$-helical conformation for **10** similar to those reported earlier in much longer peptides (S7.).[22, 25, 30, 33, 47] Temperature-dependent CD spectra of **10** (pH 4, 7, 10) (Figure 4c) revealed that the R values consistently remained at ≤0.6 up to ~318 K (S7.7-12), indicating the robustness of the 3$_{10}$-helix. The highest value of R was ~0.75 at 353 K, indicating that only a

fraction of **10** transitions into the competing α-helix, even at high temperatures (S7.12.).

Interestingly, the R value is lower in aqueous buffers than in the helix-promoting solvent TFE (2,2,2-trifluoroethanol)[48] (0.49) (Figure 4b). This means that **10** already has maximum 3_{10}-helicty under aqueous conditions (S7.15). Such behaviour has earlier been observed in short constrained α-helical peptidomimetics.[13] This is also consistent with the mean molar residue ellipticities (θ_{MRE}) of both $\pi\rightarrow\pi^*$ and $n\rightarrow\pi^*$ minima in **10** (-4.23 ± 0.22, -6.71 ± 0.13 deg·cm²·dmol⁻¹) being comparable in magnitudes (at pH 4,7,10 and 288 to 358 K) (S7.6.) to those observed in long (≥8 residues) peptide with high 3_{10}-helicities[22, 25, 45, 47] studied under ambient conditions (S7.6). Thus CD data corroborate that the novel HBS constrains and stabilizes the short peptide **10** in a robust 3_{10}-helical fold, under a wide range of pH and temperatures.

Finally in order to examine the influence of planarization rendered by the unique exo-cyclic Moc group in current HBS model, towards stabilization of 3_{10}-helical conformation in the single unconstrained turn in **10**, **11** (cyclo[Ala[1]-Phe[2]]-Gly[3]-Val[4]-Glu[5]-Ipr[6]) was synthesized by acidic cleavage of the Moc group from **10** (Scheme 1). In the CD spectrum of **11** (pH 7), both $\theta_{\pi\rightarrow\pi^*}$ and $\theta_{n\rightarrow\pi^*}$ are halved (compared to **10**) (Figure 4d), indicating a 50% lose in fraction of 3_{10}-helical structure in **11**. There is concomitant large red-shift of $\lambda_{\pi\rightarrow\pi^*}$ (9 nm) which, although is expected since the chiroptic properties of such short helices need not resemble those of long helices,[13] indicates the distortion away from the canonical 3_{10}-helix, that is observed in **10**. Thus the structural constraint from Moc in the current HBS model induces greater 3_{10}-helicity. We are currently investigating the propensity of this HBS model to propagate the 3_{10}-helical structure in longer natural peptide sequences (>1 unconstrained turn).

In summary, substitution of an i+3→i peptide hydrogen bond at the N-terminus of a disordered pentapeptide exclusively based on coded α-amino acids with a propyl linker and carbamylation of its N-terminal nitrogen yields the shortest constrained 3_{10}-helix which imposes 3_{10}-helicity in a short peptide sequence appended to its C-terminus. The structural stability of the 3_{10}-helix is robust over a large pH range, as confirmed by NMR and CD spectral data. Current strategy allows first access to the shortest 3_{10}-helix without need for C^{α}-tetrasubstituted α-amino acids and with complete conservation of the constrained sequence, which is crucial for recognition. Current HBS model will hence find broader applications as a tool in chemical biology.

References and notes

1. Karle, I.; Flippen-Anderson, J.; Uma, K.; Balaram, P. *Biopolymers* **1993**, *33*, 401.
2. Aravinda, S.; Shamala, N.; Roy, R. S.; Balaram, P. *J. Chem. Sci*. **2003**, *115*, 373.
3. Enkhbayar, P.; Hikichi, K.; Osaki, M.; Kretsinger, R. H.; Matsushima, N. *Proteins: Struct., Funct., Bioinf.* **2006**, *64*, 691.
4. Toniolo, C.; Benedetti, E. *Trends Biochem. Sci.* **1991**, *16*, 350.
5. Vieira-Pires, R. S.; Morais-Cabral, J. H. *J. Gen. Physiol*. **2010**, *136*, 585.
6. Schievano, E.; Bisello, A.; Chorev, M.; Bisol, A.; Mammi, S.; Peggion, E. *J. Am. Chem. Soc.* **2001**, *123*, 2743.
7. Cabezas, E.; Satterthwait, A. C. *J. Am. Chem. Soc* **1999**, *121*, 3862.
8. Chapman, R. N.; Dimartino, G.; Arora, P. S. *J. Am. Chem. Soc.* **2004**, *126*, 12252.
9. Jackson, D. Y.; King, D. S.; Chmielewski, J.; Singh, S.; Schultz, P. G. *J. Am. Chem. Soc.* **1991**, *113*, 9391.
10. Flint, D. G.; Kumita, J. R.; Smart, O. S.; Woolley, G. A. *Chem. Biol.* **2002**, *9*, 391.
11. Blackwell, H. E.; Grubbs, R. H. *Angew. Chem. Int. Ed.* **1998**, *37*, 3281.
12. Ösapay, G.; Taylor, J. W. *J. Am. Chem. Soc.* **1992**, *114*, 6966.
13. Shepherd, N. E.; Hoang, H. N.; Abbenante, G.; Fairlie, D. P. *J. Am. Chem. Soc.* **2005**, *127*, 2974.
14. Albert, J. S.; Hamilton, A. D. *Biochemistry* **1995**, *34*, 984.
15. Huyghues-Despointes, B.; Scholtz, J. M.; Baldwin, R. L. *Protein Sci.* **1993**, *2*, 80.
16. Tsou, L. K.; Tatko, C. D.; Waters, M. L. *J. Am. Chem. Soc.* **2002**, *124*, 14917.
17. Ma, M. T.; Hoang, H. N.; Scully, C. C. G.; Appleton, T. G.; Fairlie, D. P. *J. Am. Chem. Soc.* **2009**, *131*, 4505.
18. Ernst, J. T.; Becerril, J.; Park, H. S.; Yin, H.; Hamilton, A. D. *Angew. Chem. Int. Ed.* **2003**, *115*, 553.
19. Jacobsen, Ø.; Maekawa, H.; Ge, N.-H.; Görbitz, C. H.; Rongved, P.; Ottersen, O. P.; Amiry-Moghaddam, M.; Klaveness, J. *J. Org. Chem.* **2011**, *76*, 1228.
20. Jacobsen, Ø.; Klaveness, J.; Ottersen, O. P.; Amiry-Moghaddam, M. R.; Rongved, P. *Org. Biomol. Chem.* **2009**, *7*, 1599.
21. Blackwell, H. E.; Sadowsky, J. D.; Howard, R. J.; Sampson, J. N.; Chao, J. A.; Steinmetz, W. E.; O'Leary, D. J.; Grubbs, R. H. *J. Org. Chem.* **2001**, *66*, 5291.
22. Boal, A. K.; Guryanov, I.; Moretto, A.; Crisma, M.; Lanni, E. L.; Toniolo, C.; Grubbs, R. H.; O'Leary, D. J. *J. Am. Chem. Soc.* **2007**, *129*, 6986.
23. Madden, M. M.; Vera, C. I. R.; Song, W.; Lin, Q. *Chem. Commun.* **2009**, 5588.
24. Ousaka, N.; Sato, T.; Kuroda, R. *J. Am. Chem. Soc*. **2008**, *130*, 463.
25. Biron, Z.; Khare, S.; Samson, A. O.; Hayek, Y.; Naider, F.; Anglister, J. *Biochemistry* **2002**, *41*, 12687.
26. Fiori, W. R.; Miick, S. M.; Millhauser, G. L. *Biochemistry* **1993**, *32*, 11957.
27. Karle, I. L.; Flippen-Anderson, J. L.; Uma, K.; Balaram, H.; Balaram, P. *Proc. Natl. Acad. Sci. U.S.A.* **1989**, *86*, 765.
28. Shamala, N.; Nagaraj, R.; Balaram, P. *Biochem. Biophys. Res. Commun.* **1977**, *79*, 292.
29. Karle, I. L.; Flippen-Anderson, J. L.; Uma, K.; Balaram, H.; Balaram, P. *Proc. Natl. Acad. Sci. U.S.A.* **1989**, *86*, 765.
30. Toniolo, C.; Polese, A.; Formaggio, F.; Crisma, M.; Kamphuis, J. *J. Am. Chem. Soc.* **1996**, *118*, 2744.
31. Toniolo, C.; Crisma, M.; Moretto, A.; Peggion, C.; Formaggio, F.; Aleman, C.; Cativiela, C.; Ramakrishnan, C.; Balaram, P. *Chem. Eur. J.* **2015**, *21*, 13866.
32. Gessmann, R.; Brückner, H.; Aivaliotis, M.; Petratos, K. *J. Pept. Sci.* **2015**, *21*, 476.
33. Formaggio, F.; Crisma, M.; Rossi, P.; Scrimin, P.; Kaptein, B.; Broxterman, Q. B.; Kamphuis, J.; Toniolo, C. *Chem. Eur. J.* **2000**, *6*, 4498.
34. Patgiri, A.; Jochim, A. L.; Arora, P. S. *Acc. Chem. Res.* **2008**, *41*, 1289.
35. Wang, D.; Liao, W.; Arora, P. S. *Angew. Chem. Int. Ed.* **2005**, *44*, 6525.
36. Chapman, R.; Kulp, I., John L; Patgiri, A.; Kallenbach, N. R.; Bracken, C.; Arora, P. S. *Biochemistry* **2008**, *47*, 4189.
37. Muñoz, V.; Serrano, L. *Nat. Struct. Mol. Biol.* **1994**, *1*, 399.
38. Kan, T.; Fukuyama, T. *Chem. Commun.* **2004**, 353.
39. Barlow, D.; Thornton, J. *J. Mol. Biol.* **1988**, *201*, 601.
40. Sudha, T.; Vijayakumar, E.; Balaram, P. *Chem. Biol. Drug. Des.* **1983**, *22*, 464.
41. Wishart, D. S.; Sykes, B. D. In *[12] Chemical shifts as a tool for structure determination*; Academic Press, 1994; Vol. 239. pp 363.
42. Karplus, M. *J. Am. Chem. Soc* **1963**, *85*, 2870.
43. Perutz, M. *Nature* **1951**, *167*, 1053.
44. Pal, L.; Basu, G. *Protein Eng.* **1999**, *12*, 811.
45. Yoder, G.; Polese, A.; Silva, R.; Formaggio, F.; Crisma, M.; Broxterman, Q. B.; Kamphuis, J.; Toniolo, C.; Keiderling, T. A. *J. Am. Chem. Soc.* **1997**, *119*, 10278.
46. Manning, M. C.; Woody, R. W. *Biopolymers* **1991**, *31*, 569.
47. Moretto, A.; Formaggio, F.; Kaptein, B.; Broxterman, Q. B.; Wu, L.; Keiderling, T. A.; Toniolo, C. *Peptide Science* **2008**, *90*, 567.
48. Luidens, M. K.; Figge, J.; Breese, K.; Vajda, S. *Biopolymers* **1996**, *39*, 367.

Hydrogen bond surrogate stabilized water soluble 3_{10}-Helix from a disordered pentapeptide containing coded α-amino acids

Sunit Pal, Erode N. Prabhakaran*

Department of Organic Chemistry, Indian Institute of Science, Karnataka, Bangalore, India – 560 012.

Highlights

1. **First covalent H-bond surrogate (HBS) for i+3→i peptide main chain H-bond rationally designed.**
2. **Method developed to insert it at N-terminus of a disordered pentapeptide with natural α-amino acids**.
3. **2D NMR and CD show the HBS-pentapeptide adopts robust 3_{10}-helix with thermal and pH stability.**
4. **Planarization of N-terminal residue by Moc group influences 3_{10}-helix stability.**
5. **The 3_{10}-helical peptide is uniquely water soluble.**

* Corresponding author. Tel.: +91-80-2293-3380; fax: +91-80-2360-0529; e-mail: erodeprabhakaran02@gmail.com